Synthesis and Properties of Noncoplanar Rigid-rod Aromatic Polyamides Containing Phenyl or Naphthyl Substituents

Guey-Sheng Liou[1],*, Yi-Kai Fang[1] and Hung-Ju Yen[1]

[1]*Functional Polymeric Materials Research Laboratory, Department of Applied Chemistry,
National Chi Nan University, 1 University Road, Puli, Nantou Hsien, 54561 Taiwan, Republic of China
(*Author for correspondence; Tel.: +88-6492-910960; Fax: +88-6492-917956; E-mail: gsliou@ncnu.edu.tw)*

Abstract

A series of novel aromatic polyamides having noncoplanar biphenylene units in the main chain and bulky naphthyl or phenyl pendant group at 2,2′-disubstituted position were prepared from the two rigid-rod aromatic dicarboxylic acid monomers, 2,2′-diphenylbiphenyl-4,4′-dicarboxylic acid (**1**) and 2,2′-dinaphthylbiphenyl-4,4′-dicarboxylic acid (**2**), and various aromatic diamines. These polyamides were readily soluble in many organic solvents and showed excellent thermal stability associated with high glass-transition temperatures in the range of 229–292°C. These polymers also exhibited strong UV–Vis absorption bands at 262–353 nm in NMP solution, and their photoluminescence spectra showed maximum bands at 440–462 nm in the purple to blue region. The poly(amine–amide) **IId** derived from the diamine with triphenylamine moieties revealed excellent electrochromic contrast and coloration efficiency, changing color from the pale yellowish neutral form to green then to the blue oxidized forms when scanning potentials positively from 0.00 to 1.30 V.

Introduction

Rigid-rod aromatic polyamides and polyimides have become an important area of study because of their unique mechanical, thermal, and morphological properties [1–7]. However, rigidity of the backbone and strong hydrogen bonding results in high melting or glass transition temperatures (Tg's) and insolubility in common organic solvents [8–10]. Therefore, a great deal of effort has been expended to improve the processing characteristics of the relatively intractable polymer. One of the successful approaches to increase solubility of the rod-like polymers included the use of bulky flateral substituents [11–17], flexible alkyl side chains [18, 19], unsymmetrical [20–22], alicyclic [23], and kinked structure [24–27]. To develop processable high-performance materials, polymer structure modification that increase the solubility while maintaining the rigid-rod character and the thermal stability are of particular interest.

Another approach employed to increase optical transparency and improve solubility of rigid-rod polyamides and polyimides is by incorporation of the noncoplanar conformation into polymer backbone. In the past studies [28–35], polyamides and polyimides by adding substituents at the 2- and 2′-positions such as methyl, cyano, trifluoromethyl, methyl-substituted phenyl, halogen, methacrylate, sulfonic acid, and trifluoromethylphenoxy groups of the biphenyl moiety appeared to force the two substituted groups into a noncoplanar conformation. The bulky phenyl and naphthyl units incorporated at the 2,2′-substituted position of biphenylene as pendant groups could efficiently disrupt the crystal packing and increase solubility and high optical transparency of polymers [36–38]. This article reports the synthesis of two series of newly rigid-rod aromatic polyamides from rigid-rod aromatic dicarboxylic acids bearing pendent phenyl and naphthyl units, 2,2′-diphenyl-biphenyl-4,4′-diacrboxylic acid and 2,2′-dinaphthylbi-phenyl-4,4′-diacrboxylic acid, respectively. The general properties such as solubility, crystallinity and thermal properties are reported. The photophysical and electro-chemical properties of some typical polymers prepared by casting solution onto an indium–tin oxide (ITO)-coated glass substrate are also described herein.

Experimental section

General directions

Two phenyl- and naphthyl-substituted rigid-rod aromatic dicarboxylic acid monomers, 2,2′-diphenylbiphenyl-4,4′-dicarboxylic acid (**1**) and 2,2′-di(1-naphthyl)biphenyl-4, 4′-dicarboxylic acid (**2**), were synthesized by the Suzuki coupling reaction of 2,2′-diiodobiphenyl-4,4′-dicarboxylic acid dimethyl ester with benzeneboronic acid and naph-

TPP, Pyridine

NMP, CaCl$_2$

Ar:

a   b   c   d

e   f   g
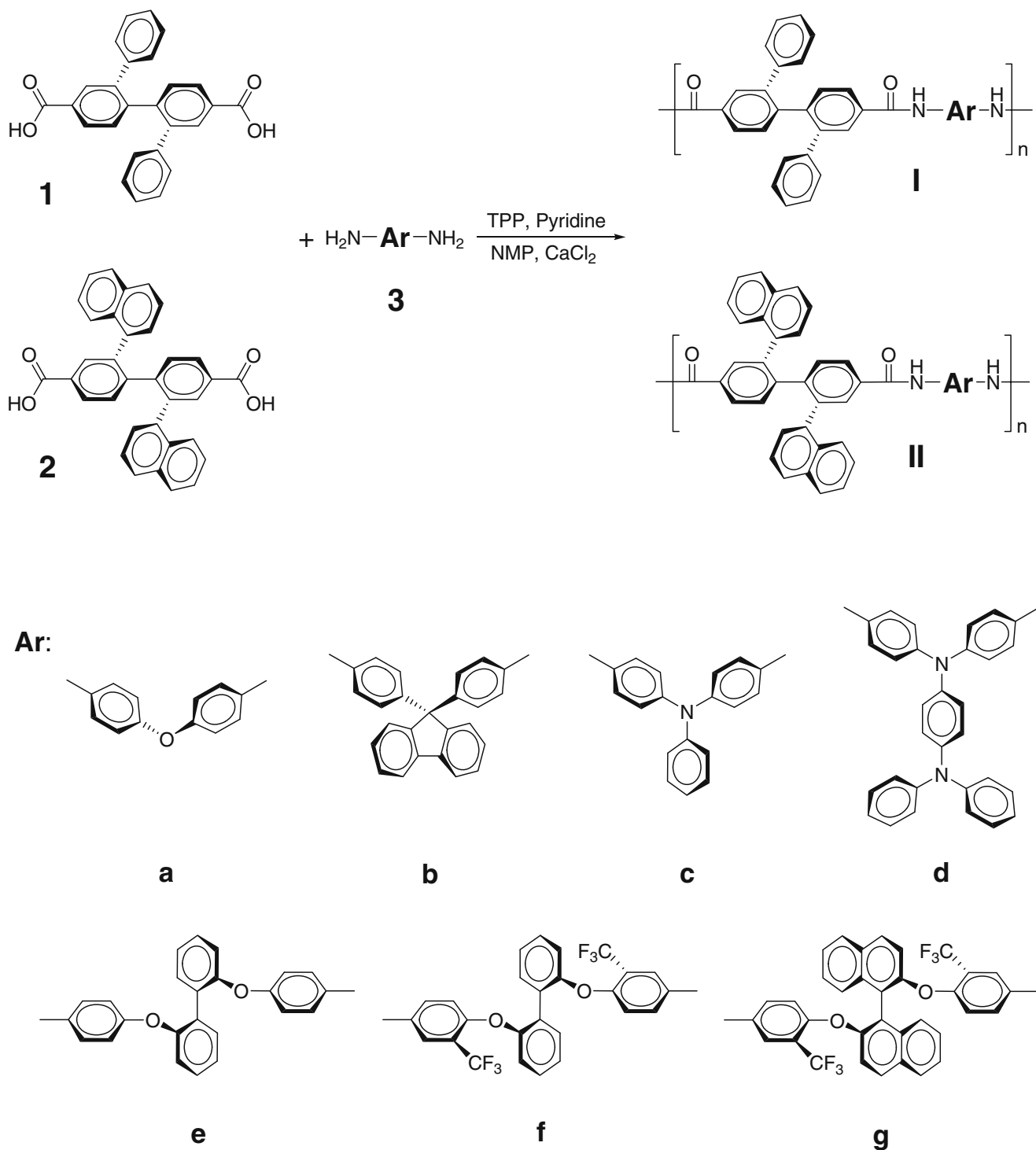
Scheme 1. Synthesis of polyamides.

thaleneboronic acid, respectively, followed by alkaline hydrolysis of the ester groups [38]. Commercially available aromatic diamines such as 4,4′-oxydianiline (**3a**) (TCI), and 9,9-bis(4-aminophenyl)fluorene (**3b**) (TCI) were used as received. 4,4′-Diaminotriphenylamine [39] (**3c**), *N,N*-bis(4-aminophenyl)-*N′,N′*-diphenyl-1,4-phenylenediamine [40] (**3d**), 2,2′-bis(4-aminophenoxy)-biphenyl [41] (**3e**), 2,2′-bis(4-amino-2-trifluoromethylphenoxy)-biphenyl [6] (**3f**), 2,2′-bis(4-amino-2-trifluoromethylphenoxy)-1,1′-binaphthyl [6] (**3g**) were synthesized according to reported procedure. Commercially obtained anhydrous calcium

chloride (CaCl$_2$) was dried under vacuum at 180°C for 8 h. Tetrabutylammonium perchlorate (TBAP) (Acros) was recrystallized twice from ethyl acetate and then dried in vacuo prior to use. All other reagents were also used as received from commercial sources.

Infrared spectra were recorded on a PerkinElmer RXI FT-IR spectrometer. ^{1}H and ^{13}C NMR spectra were measured on a Bruker Avance 500 MHz FT-NMR system and referenced to the DMSO-d_6 signal, and peak multiplicity was reported as follows: s, singlet; d, doublet; t, triplet. Elemental analyses were run in an Elementar

Table 1. Inherent viscosity and GPC data of the polyamides

Code	$\eta_{inh}{}^a$ (dl/g)	$M_n{}^b$	$M_w{}^b$	M_w/M_n
Ia	0.31	–c	–	–
Ib	0.37	–	–	–
Ic	0.35	–	–	–
Id	0.36	21,000	27,000	1.27
Ie	0.23	15,000	17,000	1.18
If	0.24	15,000	18,000	1.17
Ig	0.24	16,000	19,000	1.19
IIa	1.09	–	–	–
IIb	0.44	–	–	–
IIc	0.38	–	–	–
IId	0.63	23,000	31,000	1.31
IIe	0.31	20,000	24,000	1.22
IIf	0.30	21,000	26,000	1.24
IIg	0.17	12,000	13,000	1.13

a Measured at a polymer concentration of 0.5 g/dl in NMP at 30°C.
b Relative to polystyrene Standards, with THF as the elute.
c Insoluble in THF.

VarioEL-III. The inherent viscosities were determined at 0.5 g/dL concentration using a Tamson TV-2000 viscometer at 30°C. Wide-angle X-ray diffraction (WAXD) measurements of the polymer films were performed at room temperature (ca. 25°C) on a Shimadzu XRD-7000 X-ray diffractometer (40 kV, 20 mA) with a graphite monochromator, using nickel-filtered Cu–Ká radiation. Thermogravimetric analysis (TGA) was conducted with a PerkinElmer Pyris 1 TGA. Experiments were carried out
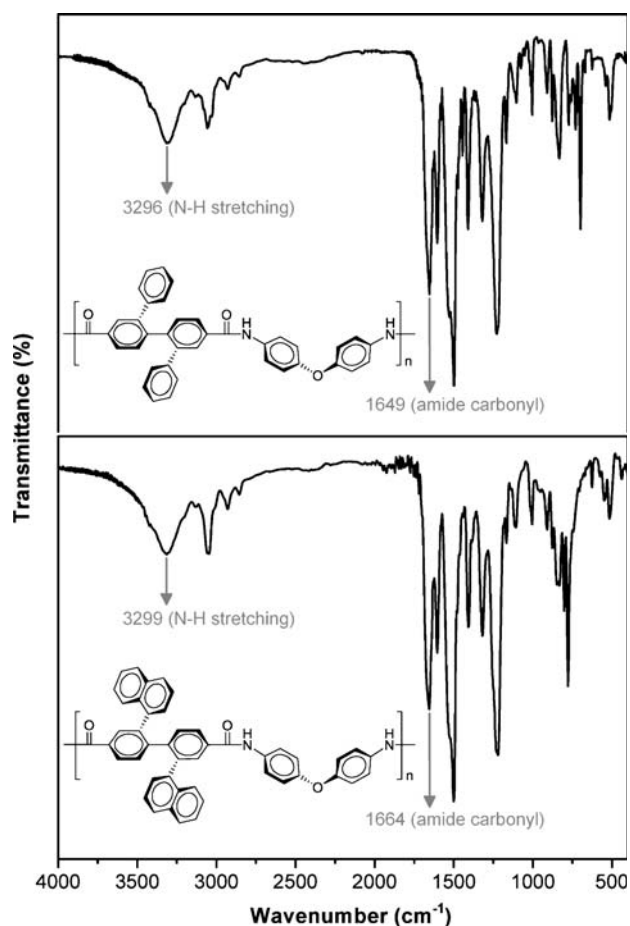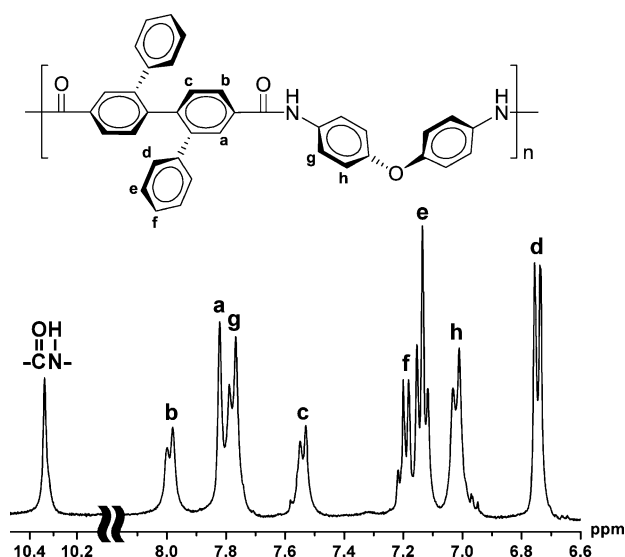

Figure 2. ^{1}H NMR spectra of polyamide **Ia** in DMSO-d_6.

on approximately 6–8 mg film samples heated in flowing nitrogen or air (flow rate=30 cm³/min) at a heating rate of 20°C/min. DSC analyses were performed on a PerkinElmer Pyris 1 DSC at a scan rate of 20°C/min in flowing nitrogen (30 cm³/min). Thermomechanical analysis (TMA) was conducted with a PerkinElmer Diamond TMA instrument. The TMA experiments were conducted from 50 to 350°C at a scan rate of 10°C/min with a penetration probe 1.0 mm in diameter under an applied constant load of 50 mN. Softening temperatures (T_s) were taken as the onset temperatures of probe displacement on the TMA traces. Ultraviolet–visible (UV–Vis) spectra of the polymer films were recorded on a Varian Cary 50 Probe spectrometer. Absorption spectra were measured with a HP 8453 UV–Visible spectrophotometer. Photoluminescence spectra were measured with a Jasco FP-6300 spectrofluorometer. Fluorescence quantum yield (Φ_F) of the samples in NMP were measured by using quinine sulfate in 1N H_2SO_4 as a reference standard (Φ_F=0.546). All corrected fluorescence

Table 2. Solubility of aromatic polyamides

Code	Solvent						
	NMP	DMAc	DMF	DMSO	*m*-cresol	THF	CHCl$_3$
Ia	++	++	++	++	++	–	–
Ib	++	++	++	++	++	–	–
Ic	++	++	++	++	++	–	–
Id	++	++	++	++	++	++	–
Ie	++	++	++	++	++	++	–
If	++	++	++	++	++	++	±
Ig	++	++	++	++	++	++	±
IIa	++	++	++	++	++	–	–
IIb	++	++	++	++	++	–	–
IIc	++	++	++	++	++	–	–
IId	++	++	++	++	++	++	–
IIe	++	++	++	++	++	++	–
IIf	++	++	++	++	++	++	±
IIg	++	++	++	++	++	++	±

Solubility ++, soluble at room temperature; ±, partially soluble or swelling on heating; −, insoluble even on heating.

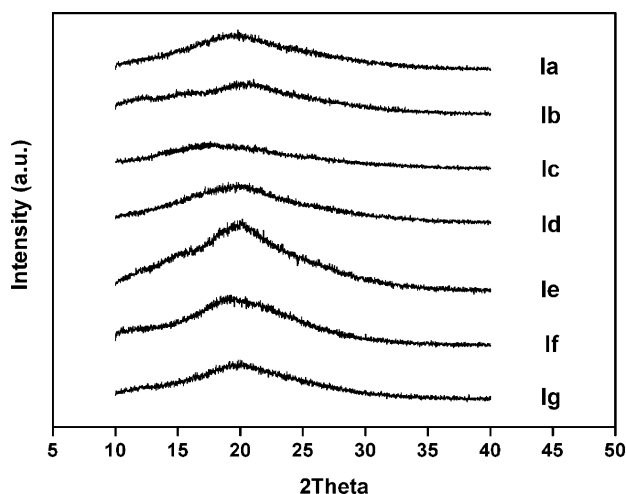*Figure 1.* IR spectrum of polyamide **Ia** and **IIa** films.

Figure 3. WAXD pattern of polyamide **I** series (film state).

excitation spectra were found to be equivalent to their respective absorption spectra. Electrochemistry was performed with a CHI 611B electrochemical analyzer. Voltammograms are presented with the positive potential pointing to the left and with increasing anodic currents pointing downwards. Cyclic voltammetry was performed with the use of a three-electrode cell in which ITO (polymer films area about 0.7×0.5 cm) was used as a working electrode and a platinum wire as an auxiliary electrode at a scan rate of 100 mV/s against a Ag/AgCl reference electrode in acetonitrile (CH_3CN) solution of 0.1 M tetrabutylammonium perchlorate (TBAP) under nitrogen atmosphere for oxidation measurement. The spectroelectrochemical cell was composed of a 1 cm cuvette, ITO as a working electrode, a platinum wire as an auxiliary electrode, and a home-made Ag/AgCl, KCl (sat.) reference electrode.

Synthesis of polyamides

The synthesis of polyamide **Ia** is used as an example to illustrate the general synthetic route. A mixture of 0.394 g (1.0 mmol) of 2,2′-diphenylbiphenyl-4,4′-dicarboxylic acid
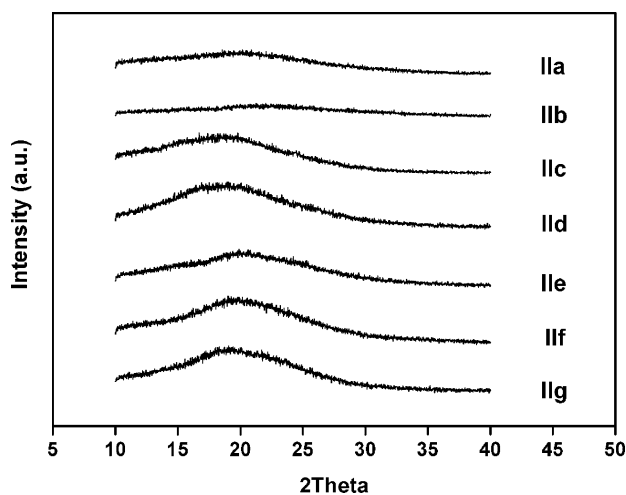

Figure 4. WAXD pattern of polyamide **II** series (film state).

(**1**), 0.200 g (1.0 mmol) of 4,4′-diaminodiphenyl ether (**3a**), 0.12 g of calcium chloride, 0.72 mL of triphenyl phosphite (TPP), 0.48 mL of pyridine, and 2.0 mL of NMP was heated with stirring at 105°C for 3 h. The obtained polymer solution was poured slowly into 200 ml of stirring methanol giving rise to a stringy, fiber-like precipitate that was collected by filtration, washed thoroughly with hot water and methanol, and dried under vacuum at 100°C. Precipitations from DMAc into methanol were carried out twice for further purification. The inherent viscosity of the obtained polyamides **Ia** was 0.31 dL/g, measured at a concentration of 0.5 g/dL in DMAc at 30°C. The IR spectrum of **Ia** (film) exhibited characteristic amide absorption bands at 3,296 cm^{-1} (N–H stretching), 1,649 cm^{-1} (amide carbonyl). ^1H NMR (DMSO-d_6, δ, ppm): 6.75 (d, 4H, H_d), 7.02 (d, 4H, H_h), 7.14 (t, 4H, H_e), 7.19 (d, 2H, H_f), 7.54 (d, 2H, H_c), 7.78 (d, 4H, H_g), 7.82 (s, 2H, H_a), 7.99 (d, 2H, H_b), 10.34 (amide–NH). Elem. Anal. Calcd. (%) for $(C_{38}H_{26}N_2O_3)_n$ $(558.62)_n$: C, 81.70; H, 4.69; N, 5.01. Found: C, 81.55; H, 4.82; N, 5.07.

Film preparation

A solution of polymer was made by dissolving about 0.50 g of the polyamide sample in 6 ml of DMAc. The homogeneous solution was poured into a 5-cm glass Petri dish, which was heated at 50°C for 1 h, 100°C for 2 h, and 160°C for 5 h to slowly release the solvent under vacuum. The obtained films were about 40–80 μm in thickness and were used for X-ray diffraction measurements, solubility tests, optical properties and thermal analyses.

Results and discussion

Basic characterization

According to the phosphorylation technique first described by Yamazaki and coworker [42, 43], two series of novel polyamides **Ia**–**Ig** and **IIa**–**IIg** with side chain phenyl or naphthyl substituted units were synthesized from the diacids, 2,2′-diphenylbiphenyl-4,4′-dicarboxylic acid and 2,2′-dinaphthylbiphenyl-4,4′-dicarboxylic acid, respectively, and various diamine as showed in Scheme 1. The polymerization was homogeneously throughout the reaction and afforded highly viscous polymer solutions. The obtained polyamides had inherent viscosities in the range of 0.17–1.09 dL/g, and the weight-average molecular weights (M_w) and number-average molecular weights (M_n) were recorded in the range of 13,000–31,000 and 12,000–23,000, respectively, relative to polystyrene standards (Table 1).

The formation of polyamides was confirmed by IR and NMR spectroscopy. Figure 1 showed a typical IR spectrum for polyamides **Ia** and **IIa**, which exhibited characteristic IR absorption bands of the amides group around 3,296 and 3,299 (N–H stretching), 1,649 and 1,664 cm^{-1} (amide carbonyl), respectively. As a typical example, the structure

Table 3. Thermal properties of polyamides

Code	T_g (°C)[a]	T_s (°C)[b]	T_d at 5% weight loss(°C)[c]		T_d at 10% weight loss(°C)[c]		Char yield (wt %)[d]
			N_2	Air	N_2	Air	N_2
Ia	277	268	480	470	525	530	67
Ib	–	285	500	515	530	555	66
Ic	271	263	445	425	555	520	74
Id	264	254	505	490	575	570	68
Ie	229	–	480	480	545	540	64
If	284	–	455	450	505	495	62
Ig	250	–	435	420	495	475	61
IIa	275	269	510	495	595	560	77
IIb	–	276	480	485	550	550	71
IIc	292	276	515	515	600	605	79
IId	283	267	530	525	600	605	76
IIe	255	–	515	510	575	575	66
IIf	272	–	480	465	525	520	65
IIg	271	–	425	425	505	500	64

The polymer film sample were heated at 300°C for 1 h prior to all the thermal analyses.
[a] Midpoint temperature of baseline shift on the second DSC heating trace (rate 20°C/min) of the sample after quenching from 400°C.
[b] Softening temperature measured by TMA with a constant applied load of 10 mN at a heating rate of 10°C/min.
[c] Decomposition temperature, recorded via TGA at a heating rate of 20°C/min and a gas flow rate of 30 cm³/min.
[d] Residual weight percentages at 800°C under nitrogen flow.

of polyamide **Ia** was also confirmed by solution NMR. Figure 2 shows a typical ^{1}H NMR spectrum of polyamide **Ia** in DMSO-d_6; all the peaks have been readily assigned to the hydrogen atoms of recurring unit.

The solubility behavior of aromatic polyamides **I** and **II** series were tested qualitatively, and the results are presented in Table 2. These polymers exhibited good solubility in common organic solvents such as NMP, DMAc, DMSO, DMF and m-cresol. The polyamides derived from diamines **3d**–**3g** were even soluble in THF. The enhanced solubility can be attributed to the introduction of bulky side chain phenyl and naphthyl-substituted group in the repeat unit, which decrease inter-chain interaction and increases the free volume. Thus, the excellent solubility makes these polymers as potential candidates for practical applications by spin- or dip-coating processes. All the side chain phenyl- and naphthyl-substituted biphenyl-based rigid-rod polyamides showed typical amo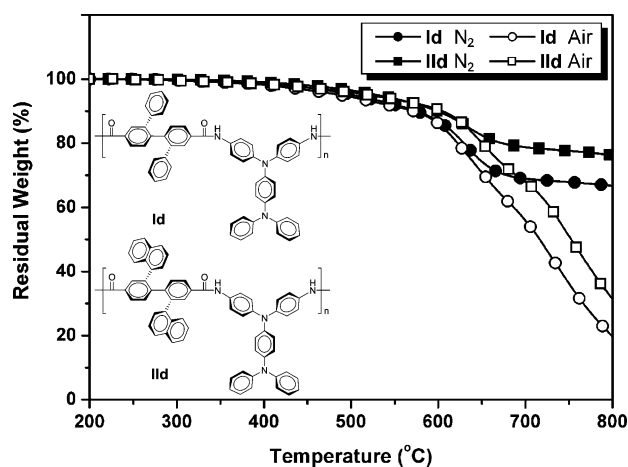rphous patterns by wide-angle X-ray diffraction diagrams (Figures 3 and 4). The amorphous nature of these phenyl and naphthyl-substituted biphenyl-based polyamides was reflected also in their good solubility.

The thermal properties of the polyamides were investigated by TGA, TMA and DSC. The results are summarized Table 3. Typical TGA curves of representative polyamides **Id** and **IId** in both air and nitrogen atmospheres are shown in Figure 5. All the aromatic polyamides exhibited good thermal stability with insignificant weight loss up to 400°C in nitrogen. The 10% weight-loss temperatures of the aromatic polyamides in nitrogen and in air were recorded in the range of 495–600 and 475–605°C, respectively. The amount of carbonized residue (char yield) of these polymer in nitrogen atmosphere was more than 61% at 800°C. The high char yields of these polymers can be ascribed to their high aromatic content. The T_g of all the aromatic polyamides could be easily measured in the DSC thermograms that were observed in the range of 229–292°C and indicated no clear melting endotherms up to the decomposition temperatures. This result supports the amorphous nature of these phenyl and
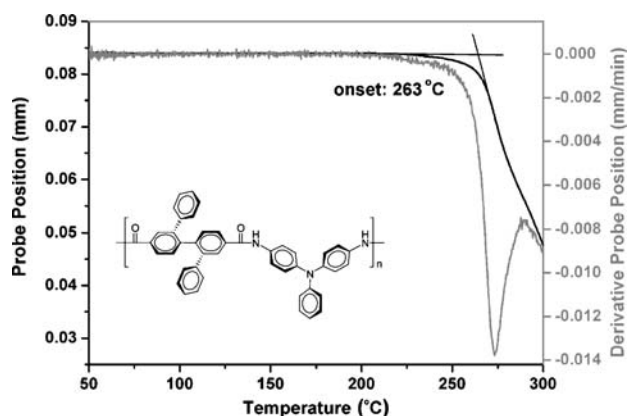

Figure 5. TGA thermograms of polyamides **Id** and **IId** at a scan rate of 20°C/min.

Figure 6. TMA curve of polyamide **Ic** with a heating rate of 10°C/min.

Table 4. Optical properties for polyamides

Index	Solutions λ(nm)[a]				Films λ(nm)				E_g^e
	Abs max	abs onset	PL max[b]	$\Phi_F{}^c$ (%)	$\lambda_0{}^d$	abs max	abs onset	PL max[b]	
Ia	263, 304	348	444	0.39	342	326	361	469	3.43
Ib	265, 310	341	452	0.36	338	323	357	462	3.47
Ic	263, 301, 350	409	460	0.42	388	343	423	521	2.93
Id	263, 306, 353	415	462	0.16	403	349	442	530	2.80
Ie	262, 300	351	440	0.33	337	318	359	465	3.45
If	263, 301	348	455	0.30	338	322	358	451	3.46
Ig	265, 298	341	460	0.22	335	320	356	452	3.48
IIa	300	351	442	0.31	345	328	365	468	3.39
IIb	299	344	453	0.26	342	321	365	451	3.39
IIc	295, 349	409	446	0.38	373	334	428	505	2.89
IId	298, 350	420	459	0.24	403	349	444	527	2.79
IIe	296	349	453	0.20	334	319	369	457	3.36
IIf	296	341	456	0.65	323	316	363	435	3.41
IIg	296	344	457	0.86	335	319	361	437	3.43

[a] Polymer concentration of 10^{-5} mol/L in NMP.
[b] They were excited at abs_{max} for both solid and solution states.
[c] The quantum yield in dilute solution was calculated in an integrating sphere with quinine sulfate as the standard (Φ_F=0.546).
[d] The cutoff wavelengths (λ_0) from the transmission UV–Vis absorption spectra of polymer films (thickness 6–15 μm).
[e] The data were calculated from polymer film by the equation: gap=$1{,}240/\lambda_{onset}$.

naphthyl-substituted biphenyl-based polymers. The softening temperature (T_s) of the polymer film samples was determined by TMA method with a loaded penetration probe, and obtained from the onset temperature of the probe displacement on the TMA trace. Typical TMA thermograms for polyamides **Ic** is illustrated in Figure 6. In all cases, the T_s values obtained by TMA are comparable to the T_g values measured by the DSC experiments (Table 3).

Optical properties

Table 4 lists the optical properties of polyamides **I** and **II** series both in solution and in the solid state (films). The absorption bands of diacid monomer **1** exhibited peaks at 262 nm assignable to the $\pi \rightarrow \pi^*$ transition, which was contributed to the twisted structure between side chain phenyl and the main chain biphenyl aromatic rings. When these monomers were excited at the maximum absorption wavelength, the emission peaks of **1** and **2** were observed at 425 and 438 nm, respectively [38], Figure 7 shows molar absorptivity and photoluminescence spectra of polyamides **I** and **II** series measured in NMP solution (Conc.: 10^{-5} M). The aromatic polyamides **I** and **II** series exhibited fluorescence emission maxima around 440–462 and 442–459 nm in NMP solution, respectively, with fluorescence quantum yield ranging from 0.16 to 0.86%. The higher fluorescence quantum yield of aromatic polyamides **IIf**–**IIg** compared to **If**–**Ig** could be attributed to the incorporation of naphthalene chromophore. In the solid state, the UV–vis absorption and photoluminescence spectra of polyamides **I** and **II** series were nearly identical and show a maxima absorbance and emission at 316–349 and 435–530 nm, respectively. The photoluminescence of these polyamide thin films by UV irradiation (365 nm) is also shown in Figure 8. For obtaining the light-colored polyamides, the lower capability of charge transfer is indispensable. Thus, we synthesized the polyamides **Ia**, **Ib**, **Ie**–**Ig** and **IIa**, **IIb**, **IIe**–**IIg** derived from aromatic diamines without intrinsic electron-donating triphenylamine units for comparison. The transmission UV–vis spectra of polyamide films are shown in Figures 9 and 10. The cutoff wavelengths (absorption edge; λ_0) were in the range of 323–403 nm. Besides **Ic**, **Id**, **IIc**, and **IId** (373–403 nm) derived from intrinsic electron-donating trphenylamine-containing diamines, all the other polyamides **I** and **II** series showed high optical transparency in the visible light region with cutoff wavelength in the ranges of 323–345 nm.

Electrochemical properties

The electrochemical redox behavior of the polyamides was investigated by cyclic voltammetry conducted by the cast film on an ITO-coated glass substrate as working electrode in dry acetonitrile containing 0.1 M of TBAP as an electrolyte under nitrogen atmosphere. The typical cyclic
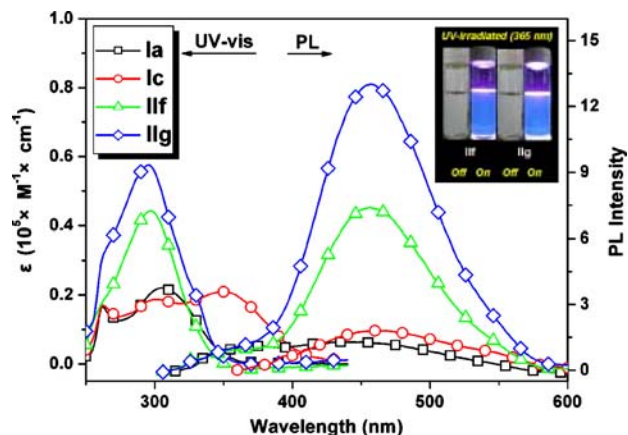

Figure 7. Molar absorptivity (*left*) and PL spectra (*right*) of polyamides **Ia**, **Ic**, **IIf** and **IIg** in NMP solution (10^{-5} M).
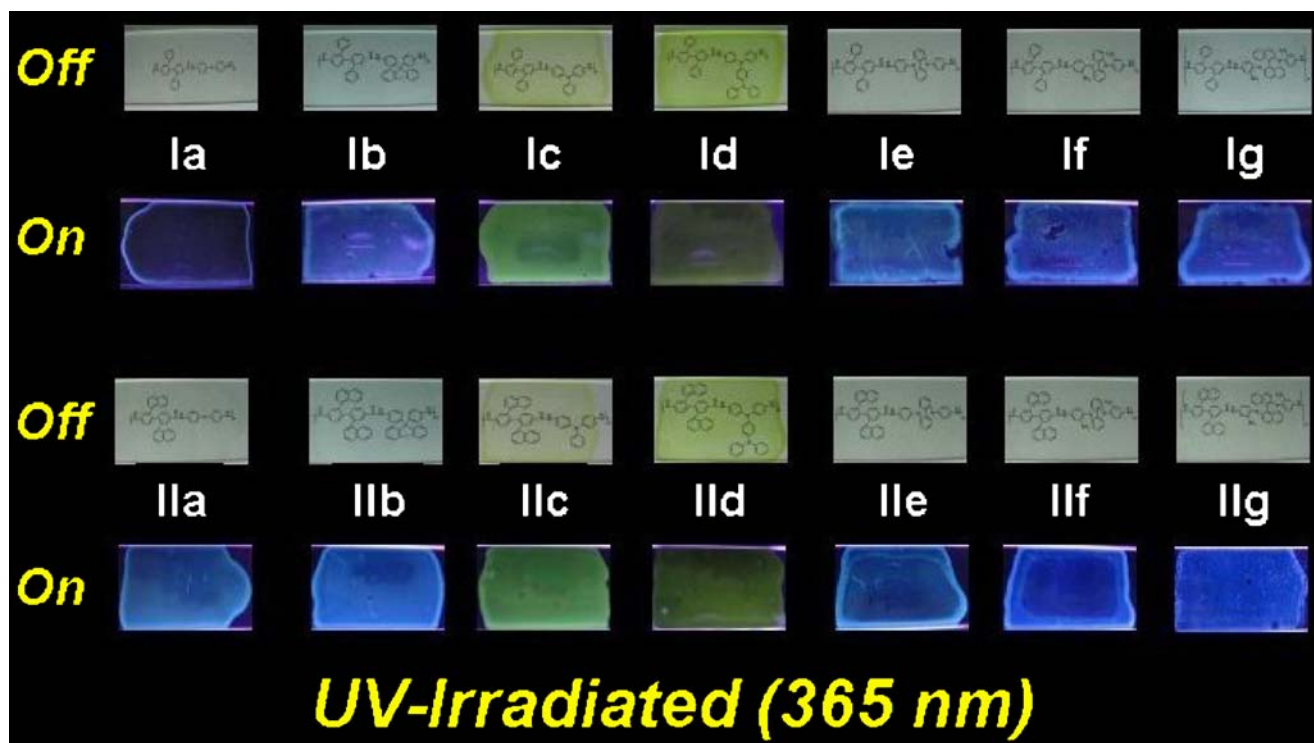
Figure 8. The photoluminescence of polymer thin films **I** and **II** series (thickness: 6–15 μm) by UV irradiation (Excited at 365 nm).

voltammograms for polyamides **Id** and **IId** are shown in Figure 11. There are two reversible oxidation redox couples at $E_{1/2}$=0.65 (E_{onset}=0.51 V) and 1.03 V, respectively. The first electron removal for polyamide **IId** is assumed to occur at the N atom surrounded by two phenyl groups with electron-donating amide linkages in the main chain, which is more electron-rich than the N atom surrounded only by two phenyl units at the side chain [39, 44]. The energy of the highest occupied molecular orbital (HOMO) and lowest unoccupied molecular orbital (LUMO) levels of polymer **IId** can be determined from the oxidation onset potential (E_{onset}) and onset absorption wavelength. The oxidation onset potential for poly(amine––amide)s **IId** has been determined as 0.51 V vs Ag/AgCl from Figure 11. The external ferrocene/ferrocenium (Fc/Fc$^+$) redox standard $E_{1/2}$ (Fc/Fc$^+$) is 0.48 V vs Ag/AgCl in CH$_3$CN. Assuming that the HOMO energy for the Fc/Fc$^+$standard is 4.80 eV with respect to the zero vacuum level, the HOMO energy for polyamide **IId** has been evaluated to be 4.83 eV.

Electrochromic characteristics

Electrochromism of the thin films from polyamide was examined by casting polymer solution onto an indium-tin oxide (ITO)-coated glass substrate, and their electrochromic transmittance spectra were monitored by a UV–vis spectrometer at different applied potentials. The electrode preparations and solution conditions were identical to those
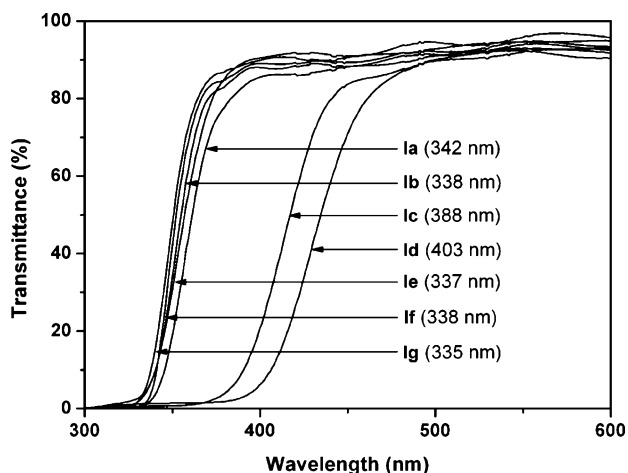

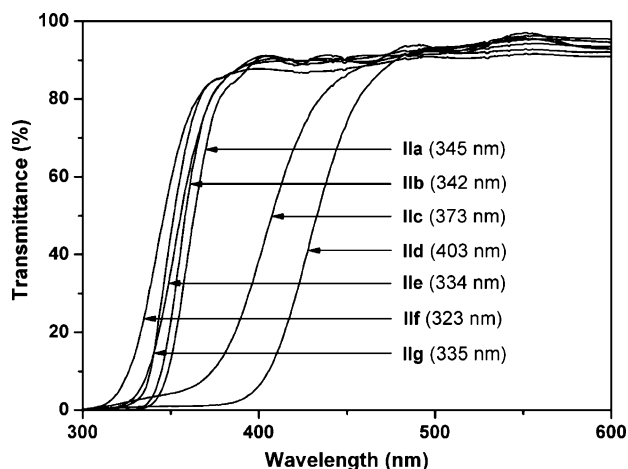*Figure 9.* UV–vis transmission spectra of polyamide **I** series films (thickness: 6–15 μm).

Figure 10. UV–vis transmission spectra of polyamide **II** series films (thickness: 6–15 μm).
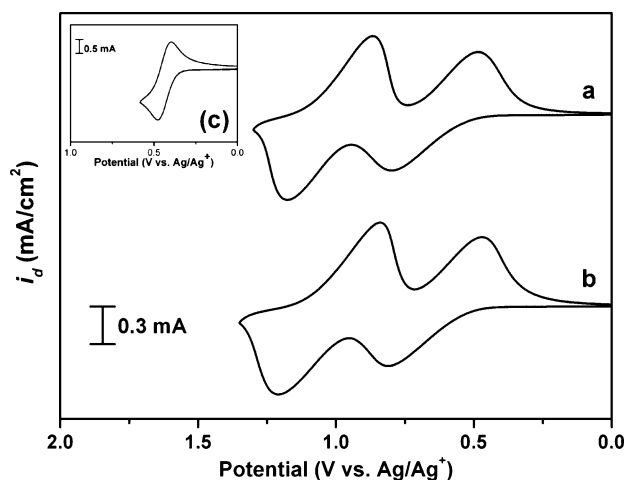
Figure 11. Cyclic voltammograms of poly(amine–amide) **a Id b IId** film onto an indium–tin oxide (ITO)-coated glass substrate and **c** ferroecne in CH$_3$CN containing 0.1 M TBAP at a Scan rate of 0.1 V/s.
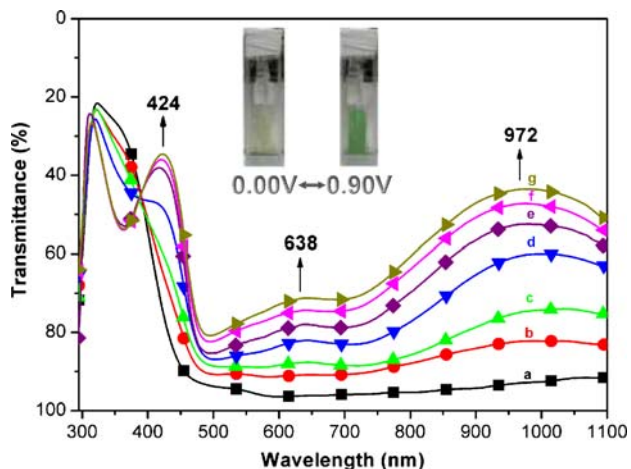

Figure 13. Electrochromic behavior of poly(amine–amide) **IId** thin film (in CH$_3$CN with 0.1 M TBAP as the supporting electrolyte) at **a** 0.95 V **b** 1.00 V **c** 1.06 V **d** 1.15 V **e** 1.30 V.

used in cyclic voltammetry. The typical electrochromic transmittance spectra of polyamides **IId** are shown as Figures 12 and 13. When the applied potentials increased positively from 0.42 to 0.90 V, the peak of characteristic absorbance at 322 nm for polyamide **IId** decreased gradually while new bands grew up at 424, 638, and 972 nm due to the first stage oxidation, and the color of the film changed from original pale yellowish to green. When the potential was adjusted to more positive values, corresponding to second stage oxidation, the spectral changes are shown as Figure 13. The characteristic peaks for poly(amine–amides)$^+$ disappeared and a new band grew up at 740 nm. The new spectrum was assigned as poly(amine–amide)$^{2+}$ and the color of the film became deep blue. Furthermore, the transmittance modulation at 972 and 740 nm having the largest contrast values, ca. 50 and 83%, are also shown in Figures 12 and 13, respectively. The coloration efficiency at 972 nm is 130 cm^2/C with high optical density change (ΔOD) up to 0.32, charge (Q) is 2.55 mC/cm^2 determined from the in situ experiments

[45]. The results presented herein also demonstrate that incorporation bulky naphthyl group into polymer side chain results in light-colored of the obtained polymers thus enhanced coloration efficiency with higher contrast of the corresponding electrochromic materials. The spectroscopic profiles and the color switching time were conducted 40 cyclic scans by applying a potential step between 0.0 to 0.90 V (Figure 14). The switching time was defined as the time that required for reach 90% of the full change in absorbance after switching potential. The **IId** would require 1.5 s at 0.90 V for switching absorbance at 424 and 972 nm and 1 s for bleaching. When the potential was set 1.30 V, thin films from poly(amine–amide) **IId** would required almost 2.5 s for coloration at 740 nm and 1.5 s for bleaching.

Figure 12. Electrochromic behavior of poly(amine–amide) **IId** thin film (in CH$_3$CN with 0.1 M TBAP as the supporting electrolyte) at **a** 0.00 V **b** 0.42 V **c** 0.50 V **d** 0.65 V **e** 0.71 V **f** 0.80 V **g** 0.90 V.
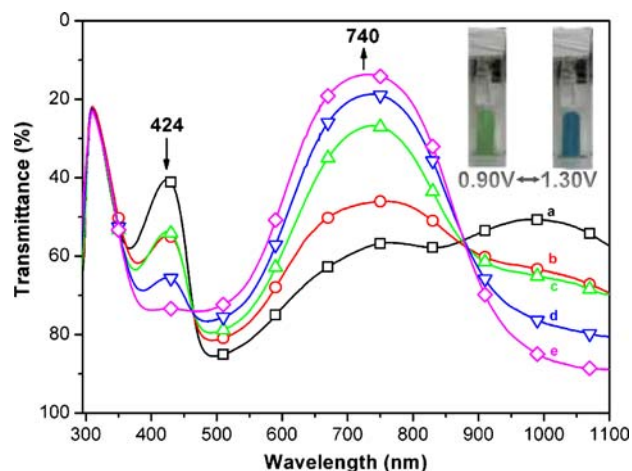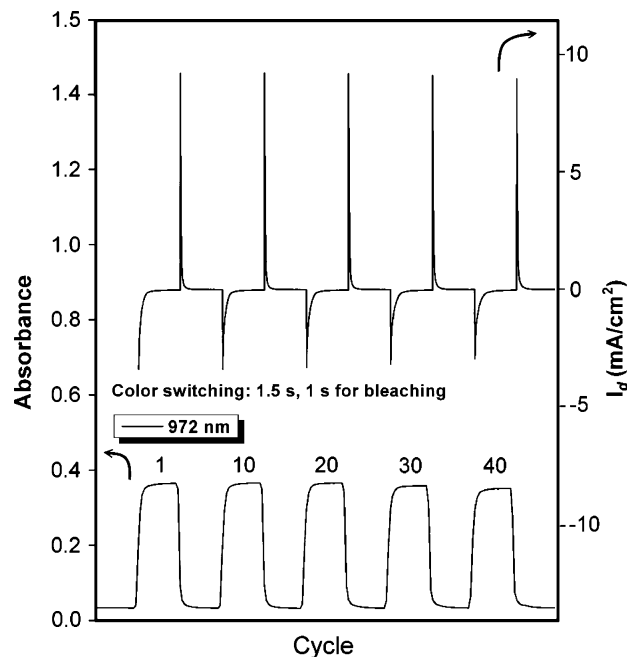

Figure 14. Potential step absorptometry of poly(amine–amide) **IId** (in CH$_3$CN with 0.1 M TBAP as the supporting electrolyte) by applying a potential step (0.00 Δ 0.90 V).

Conclusions

Two series of novel aromatic polyamides have been readily prepared from phenyl and naphthyl-substituted rigid-rod aromatic dicarboxylic acids, 2,2′-diphenylbiphenyl-4,4′-dicarboxylic acid (**1**) and 2,2′-dinaphthylbiphenyl-4,4′-dicarboxylic acid (**2**), and various aromatic diamines via the direct phosphorylation polycondensation. The introduction of the bulky phenyl and naphthyl-substituted group could increase the solubility and disrupt the copolanarity of aromatic units in chain packing and exhibited excellent thin-film-forming ability and thermal stability. In NMP solution, these aromatic polyamides **I** and **II** series exhibited fluorescence emission maxima around 440–462 and 442–459 nm, respectively. The thin films of aromatic polyamides without triphenylamine units showed high optical transparency from UV–Vis transmittance measurement with cutoff wavelength in the range of 323–345 nm. The poly(amine–amide) **IId** derived from the diamine with triphenylamine moieties revealed excellent electrochromic contrast and coloration efficiency, changing color from the pale yellowish neutral form to green then to the blue oxidized forms when scanning potentials positively from 0.00 to 1.30 V.

Acknowledgment

References

1. D.-J. Liaw, F.-C. Chang, M.-K. Leung, M.-Y. Chou and K. Muellen, *Macromolecules*, **38**, 4024 (2005).
2. H.-S. Kim, Y.-H. Kim, S.-K. Ahn and S.-K. Kwon, *Macromolecules*, **36**, 2327 (2003).
3. K.-H. Kim, S. Jang and F.-W. Harris, *Macromolecules*, **34**, 8925 (2001).
4. S.-H. Lin, F. Li, S. Z. D. Cheng and F.-W. Harris, *Macromolecules*, **31**, 2080 (1998).
5. K.-C. Chuang, J.-D. Kinder, D. L. Hull, D.-B. McConville and W.-J. Youngs, *Macromolecules*, **30**, 7183 (1997).
6. C.-P. Yang, S.-H. Hsiao, C.-Y. Tsai and G.-S. Liou, *J. Polym. Sci., A, Polym. Chem.*, **42**, 2416 (2004).
7. S.-H. Hsiao, C.-P. Yang, C.-Y. Tsai and G.-S. Liou, *Eur. Polym. J.*, **40**, 1081 (2004).
8. G.-S. Liou, S.-H. Hsiao and T.-H. Su, *J. Mater. Chem.*, **15**, 1812 (2005).
9. P.-E. Cassidy, *Thermally Stable Polymers*, Marcel Dekker, New York, 1980.
10. H.-H. Yang, *Aromatic High-strength Fibers*, Wiley, New York, 1989.
11. D.-J. Liaw and B.-Y. Liaw, *Macromol. Symp.*, **122**, 343 (1997).
12. C.-P. Yang, G.-S. Liou, C.-C. Yang and S.-H. Chen, *J. Appl. Polym. Sci.*, **78**, 1162 (2000).
13. D.-J. Liaw, P.-N. Hsu, W.-H. Chen and S.-L. Lin, *Macromolecules*, **35**, 4669 (2002).
14. G.-S. Liou and S.-H. Hsiao, *J. Polym. Sci., A, Polym. Chem.*, **40**, 1781 (2002).
15. G.-S. Liou, Y.-L. Yang and Y.-O. Su, *J. Polym. Sci., A, Polym. Chem.*, **44**, 2587 (2006).
16. G.-S. Liou, H.-W. Chen and H.-J. Yen, *J. Polym. Sci., A, Polym. Chem.*, **44**, 4108 (2006).
17. G.-S. Liou, H.-W. Chen and H.-J. Yen, *Macromol. Chem. Phys.*, **207**, 1589 (2006).
18. M. Ballauff and G.-F. Schmidt, *Macromol. Chem. Rapid. Commun.*, **8**, 93 (1987).
19. M. Steuer, M. Horth and M. Ballauff, *J. Polym. Sci., A, Polym. Chem.*, **31**, 1609 (1993).
20. L. Cheng and X.-G. Jian, *J. Appl. Polym. Sci.*, **92**, 1516 (2004).
21. G.-S. Liou, S.-H. Hsiao, W.-C. Chen and H.-J. Yen, *Macromolecules*, **39**, 6036 (2006).
22. G.-S. Liou and H.-J. Yen, *J. Polym. Sci., A, Polym. Chem.*, **44**, 6094 (2006).
23. M. Yamada, T. Matsumoto and T. Kurosaki, *Macromolecules*, **27**, 1117 (1994).
24. D.-J. Liaw, B.-Y. Liaw, P.-N. Hsu and C.-Y. Hwang, *Chem. Mater.*, **13**, 811 (2001).
25. D.-J. Liaw, B.-Y. Liaw and C.-M. Yang, *Macromolecules*, **32**, 7248 (1999).
26. C.-P. Yang, G.-S. Liou, R.-S. Chen and C.-Y. Yang, *J. Polym. Sci., A, Polym. Chem.*, **38**, 1090 (2000).
27. F. P. Glatz and R. Mulhaupt, *Polym. Bull.*, **31**, 137 (1993).
28. F. Li, S. Fang, J.-J. Ge, P. S. Honigfort, J.-C. Chen, F.-W. Harris and S. Z. D. Cheng, *Polymer*, **40**, 4571 (1999).
29. F. Li, J.-J. Ge, P.-S. Honigfort, S. Fang, J.-C. Chen, F.-W. Harris and S. Z. D. Cheng, *Polymer*, **40**, 4987 (1999).
30. K.-H. Kim, S. Jang and F.-W. Harris, *Macromolecules*, **34**, 8925 (2001).
31. J. Fang, X. Guo, S. Harada, T. Watari, K. Tanaka, H. Kita and K. I. Okamoto, *Macromolecules*, **35**, 9022 (2002).
32. T. Matsuura, S. Ando and S. Sasaki, In G. Hougham, P.-E. Gassidy, K. John and T. Davidson, (Eds.), *Fluoropolymer 2: Properties*, Plenum, New York, pp 305, 1999.
33. K. Han, H.-J. Lee and T.-H. Rhee, *J. Appl. Polym. Sci.*, **74**, 107 (1999).
34. D.-J. Liaw, B.-Y. Liaw and M.-Q. Jeng, *Polymer*, **39**, 1597 (1998).
35. D.-J. Liaw, B.-Y. Liaw, J.-R. Chen and C.-M. Yang, *Macromolecules*, **32**, 6860 (1999).
36. C.-F. Yang, H.-D. Chen, K.-H. Yang, M.-K. Leung, C.-C. Wu, C.-C. Yang, C.-C. Wang and W.-S. Fann, *Mater. Sci. Eng. B*, **85**, 236 (2001).
37. M.-K. Leung, M.-Y. Chou, Y.-O. Su, C.-L. Chiang, H.-L. Chen, C.-F. Yang, C.-C. Yang, C.-C. Lin and H.-T. Chen, *Org. Lett.*, **5**, 839 (2003).
38. G.-S. Liou, S.-H. Hsiao and Y.-K. Fang, *J. Polym. Sci., A, Polym. Chem.*, **44**, 6466 (2006).
39. Y. Oishi, H. Takado, M. Yoneyama, M. Kakimoto and Y. Imai, *J. Polym. Sci., A, Polym. Chem.*, **28**, 1763 (1990).
40. S.-H. Cheng, S.-H. Hsiao, T.-H. Su and G.-S. Liou, *Macromolecules*, **38**, 307 (2005).
41. G.-S. Liou, M. Maruyama, M. Kakimoto and Y. Imai, *J. Polym. Sci., A, Polym. Chem.*, **31**, 3273 (1993).
42. N. Yamazaki, F. Higashi and J. Kawabata, *J. Polym. Sci., Polym. Chem. Ed.*, **12**, 2149 (1974).
43. N. Yamazaki, M. Matsumoto and F. Higashi, *J. Polym. Sci., Polym. Chem. Ed.*, **13**, 1375 (1975).
44. T.-H. Su, S.-H. Hsiao and G.-S. Liou, *J. Polym. Sci., A, Polym. Chem.*, **43**, 2085 (2005).
45. R. J. Mortimer and J. R. Reynolds, *J. Mater. Chem.*, **15**, 2226 (2005).